Identifying global climate change using simple indices

David J. Karoly and Karl Braganza

Department of Mathematics and Statistics, Monash University, Clayton, Vic., Australia

Abstract. Several simple indices of surface air temperature patterns are used to describe global climate variability and change. The indices include the land-ocean temperature contrast, the hemispheric contrast, the meridional gradient, and the magnitude of the seasonal cycle, as well as the global-mean temperature. The behaviour of the indices is investigated using global observational data for the period 1881–1994 and long control and anthropogenic climate change simulations with two different climate models. The indices represent the key features of the "fingerprint" of greenhouse climate change. For natural climate variations, they contain information independent of the global-mean temperature. The observed trends over the last 40 years in all the indices, except for the hemispheric contrast, are unlikely to have occurred due to natural climate variations and all are consistent with model simulations of anthropogenic climate change.

Introduction

The possible contribution of human activity to climate change over the last century has attracted considerable interest [*Santer et al*, 1996a]. We follow the detection and attribution methodologies used in fingerprint detection studies [*Santer et al*, 1996a; *Hegerl et al*, 1997] but apply them using a small number of indices of global climate change. Appropriate indices represent the key features of the spatial patterns of surface air temperature change due to the enhanced greenhouse effect. The combination of several of these simple global indices is likely to have more power to attribute climate change than using global-mean temperature alone. While this approach may not be as statistically powerful as the fingerprint method, it should be easier to interpret. A related regional study [*Karl et al.*, 1996] defined climate change indices for the United States.

The observational and climate model datasets are described in the next section. Then, the selection of appropriate indices is discussed. Finally, the observed trends in these indices are compared with those from anthropogenic climate change simulations.

Datasets

The observed data used here are gridded surface air temperatures over land [*Jones*, 1994] and gridded ocean surface temperatures [*Parker et al.*, 1995], as used in the IPCC second assessment report [*Nicholls et al.*, 1996]. These data are used for the period 1881–1994.

A data mask was created based on the regions where there was reasonable coverage of observed data since 1910 (more than 70% of years with data). This means that regions at high latitudes in both hemispheres and over the Southern Ocean were not included. Annual values of the indices were calculated from the observations and the simulations using this mask. Values of the indices were not sensitive to variations of the data mask.

For the climate model simulations, we used surface air temperature data from two different coupled ocean--atmosphere climate models, one from CSIRO in Australia (CSIRO9) and the other from the Hadley Centre, the Meteorological Office, U.K. (HadCM2). The CSIRO9 model uses a spectral atmospheric model with 9 levels in the vertical and horizontal resolution of 3.2°lat. by 5.6°long., a gridpoint ocean model with the same horizontal resolution and 21 levels, and a dynamic sea ice model [*Gordon and O'Farrell*, 1997]. The HadCM2 model has higher resolution, using gridpoint atmospheric and ocean models with horizontal resolution of 2.5°lat. by 3.75°long. and 19 and 20 levels, respectively [*Johns et al*, 1997]. Both models include adjustments of the surface fluxes between the atmosphere and ocean to ensure a stable climate in their control simulations.

We used model simulations with three different types of external forcing:
Control: extended simulations (1000 years for CSIRO9, 990 years for HadCM2), during which the external forcing factors and greenhouse gas concentrations were fixed at current observed levels. These simulations give an estimate of the natural internal variability of the climate system.
Greenhouse gas (G): simulations with increasing carbon dioxide concentrations to give the same changes in radiative forcing as observed changes of greenhouse gases from 1880 to 1990 and projected increases from 1990 to 2100 from the IS92a scenario [*Houghton et al*, 1992].
Greenhouse gas and sulphate aerosols (GS): in addition to the greenhouse gas forcing above, the effect of increasing sulphate aerosols was included in the model simulations by regional increases in the surface albedo based on estimates of sulphate emissions [*Mitchell and Johns*, 1997]. The aerosol forcing used in the CSIRO9 model was about 30% smaller than that used in the HadCM2 model. The different sulphate forcings used in the two models are both within the range of observational estimates.

From the HadCM2 model, we had four G simulations and four GS simulations, each started from different initial conditions. From the CSIRO model, we had two G simulations and one GS simulation. Output from the model simulations was used only over fixed regions defined by the data mask.

Selection of the Indices

The selection of a small number of global indices to represent global surface temperature patterns is based on the need to retain the key features of the spatial patterns of climate change, while ensuring the maximum additional in-

Paper number 1999GL000000.
0094-8276/00/1999GL000000$05.00

Table 1. Correlations of Decadal Variations

Index	Obs	CSIRO9	HadCM2
Land T	0.79	0.90	0.94
Ocean T	0.98	0.94	0.98
Land - Ocean T	-0.05	0.54	0.55
NH T	0.94	0.95	0.94
SH T	0.87	0.69	0.87
NH - SH T	0.24	0.62	0.26
Merid. T grad.	0.24	0.40	0.44
NH DJF T	0.53	0.61	0.67
NH JJA T	0.58	0.78	0.63
Ann. cycle T	-0.17	-0.06	-0.20

Correlations of low-pass filtered global-mean surface air temperature with the other global temperature indices and components of these indices. Values in each column are calculated from linearly-detrended observations and control climate model simulations.

formation from each index. Some features of greenhouse climate change are global warming, greater warming over land than over oceans, greater warming at high latitudes than at low latitudes, and reduction in the magnitude of the annual cycle of temperature over land. Another feature is a difference in the warming between the Northern and Southern Hemispheres arising from differences in the effects of aerosols and ocean mixing. Each additional index should be almost independent of those already included, to ensure the maximum additional information content. Using the above considerations, the following indices were selected: global-mean surface air temperature (global mean); mean air temperature contrast between land and ocean (land - ocean); mean temperature contrast between Northern and Southern Hemispheres (NH - SH); mean temperature contrast between NH high latitudes (50–65°N) and subtropics (20–35°N) (meridional gradient); and mean magnitude of the annual cycle of temperature over land (ann. cycle).

There are also physical reasons for the choice of these indices, as they are associated with some of the dynamical factors determining the large-scale atmospheric circulation. The land-ocean temperature contrast determines the intensity of monsoon circulations while the meridional temperature gradient determines the strength of midlatitude weather systems [*Peixoto and Oort*, 1992].

Some of these indices have been used previously for studies of climate variability and change, including the land-ocean temperature contrast [*Jain et al*, 1999], the meridional temperature gradient [*Gitelman et al*, 1999; *Jain et al*, 1999], the magnitude of the annual cycle [*Thomson*, 1995; *Mann and Park*, 1996] and the hemispheric temperature contrast [*Kaufmann and Stern*, 1997]. However, the results from these studies have been inconsistent and no study has considered all these indices together.

An indication of the relationship between these indices for natural low-frequency climate variations is shown in Table 1. This shows the correlations between the global-mean temperature and each of the indices, together with some of the components used to generate the indices. The correlations were calculated from detrended observational data and control model data, which were filtered to retain variations with periods longer than 10 years. The observational data were detrended to try to remove the possible influence of changing human activity. This would also remove any natural century time-scale variations.

While the global-mean temperature is highly correlated with mean temperature over both the land and the oceans, the correlation with the temperature contrast between land and ocean is smaller, indicating that this index contains information independent of that in the global-mean temperature. Similarly, the correlation of global-mean temperature with the temperature contrast between the NH and SH is smaller than the correlation with the mean temperature in either hemisphere alone. The meridional temperature gradient also shows much smaller correlations with the global-mean temperature than does the NH temperature. The magnitude of the annual cycle of temperature has negligible correlations with the global-mean temperature variations. Hence, each of these indices contains information independent of the global-mean temperature for natural low-frequency variations.

The magnitude of the low-frequency internal variability simulated by the climate models is compared with the observed natural variability in Table 2 for the different indices. We might expect the variability in the observed indices to be greater than that simulated because they include the effects of natural forced variations due to volcanic eruptions or changes in solar irradiance (which are not included in the model simulations), and the residual effects of human-induced changes in forcing after the linear detrending. However, the variability of the modelled indices is similar to that observed, with the standard deviations of the indices in the Hadley Centre model always within 20% of those observed and those in the CSIRO model generally 30%–40% less than observed. Hence, the Hadley Centre model seems to provide a good estimate of the unforced variability of these simple indices on decadal time scales, in agreement with another assessment of variability simulated by this model [*Tett et al.*, 1997].

Simulated and observed climate change

The observed low-frequency variations of these indices since 1880 were compared with those in the climate model simulations with anthropogenic forcings and the control sim-

Table 2. Standard Deviations of Decadal Variations

Index	Obs	CSIRO9	HadCM2
Global mean T	0.087	0.051	0.084
Land T	0.103	0.080	0.117
Ocean T	0.085	0.044	0.075
Land - Ocean T	0.083	0.058	0.066
NH T	0.105	0.073	0.099
SH T	0.084	0.040	0.083
NH - SH T	0.087	0.068	0.078
Merid. T grad.	0.130	0.161	0.153
NH DJF T	0.186	0.130	0.173
NH JJA T	0.125	0.095	0.123
Ann. cycle T	0.132	0.095	0.122

Standard deviations of the low-pass filtered global temperature indices and components of these indices (in °C). Values in each column are calculated from linearly-detrended observations and control climate model simulations.

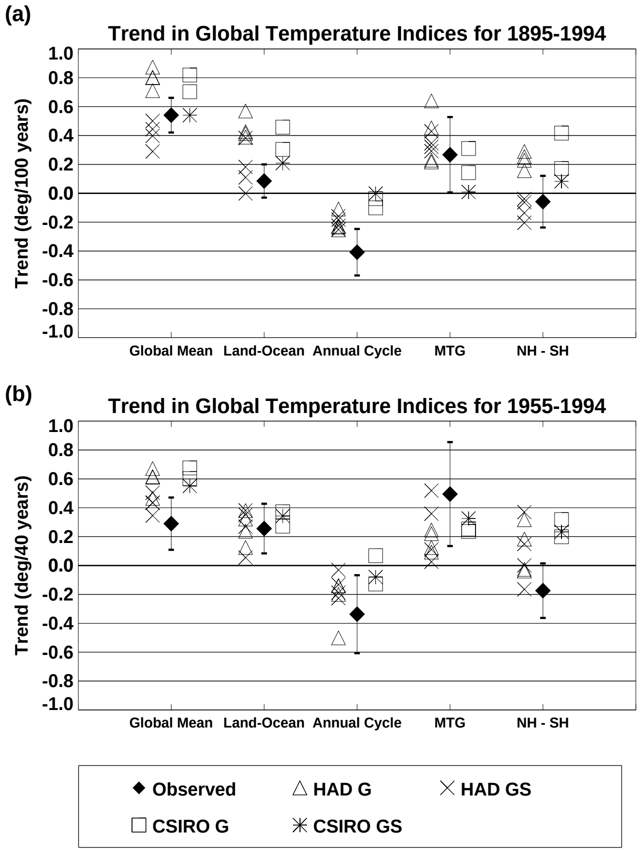

Figure 1. Trends in the five temperature indices over the periods (a) 1895–1994 and (b) 1955–94. The symbols show the trends estimated from the observational data and the individual model simulations. The uncertainty in each of the estimated trends is shown by the 90% confidence interval about the observed trend, estimated from the distribution of trends from the long HadCM2 control simulation.

ulations. For the time series of global-mean temperature, the observed warming over the last 100 years is smaller than in the model simulations with increasing greenhouse gas forcing alone, similar to that in the simulations with increasing greenhouse gas and sulphate aerosol forcing, and much greater than the variability in the unforced model simulations. The observed land-ocean temperature contrast shows a slight increase that is broadly similar to that in the forced model simulations and larger than the variability of this index in the unforced model simulations.

The linear trends in each of the indices provide a more quantitative comparison. They are shown in Figure 1 for two separate periods: 1895–1994 (last 100 years) and 1955–1994 (last 40 years) from the observational data and the forced model simulations. The shorter second period was chosen to include the time of best observational data coverage. Observed data after 1994 have not been used because the IPCC Second Assessment [*Nicholls et al.*, 1996] used data only up to 1994 and the large El Nino event in 1998 had a significant influence on the record warm global temperatures in that year.

The uncertainty in the observed trends due to internal climate variability was estimated for each of the indices from the range of trends found in the long, unforced climate model simulations. The Hadley Centre model gives a slightly larger range of trends, so it was used to provide estimates of the trend uncertainty. The different simulations with the same forcings from the Hadley Centre model also allow the uncertainty of the trends due to the chaotic nature of climate to be estimated from the forced model simulations.

First, we tried to identify significant observed trends by assessing whether they were significantly different from zero. Next, we compared the observed trends with those from the forced model simulations to assess whether the observed changes were consistent with the forced climate changes. As shown in Fig. 1, the observed trends over the period 1955–94 in all the indices, apart from the hemispheric temperature contrast, are significant and cannot be explained by natural internal climate variations (as the 90% confidence intervals about the observed trends do not include zero trend). The observed trends over the last 100 years are similar but generally significant at lower confidence levels. All the observed trends are consistent with those in model simulations forced by increasing greenhouse gases and sulphate aerosols (as the 90% confidence intervals about the observed trends include at least one of the forced model trends). This indicates that the observed climate change shown by these indices is consistent with that due to human-induced climate forcing and not consistent with natural variability alone.

The observed trends over the last 100 years and over the last 40 years agree slightly better with the simulations forced by increasing greenhouse gases and sulphate aerosols than with those forced by increasing greenhouse gases alone. The rate of change of the observed and model indices over the last 40 years is larger than over the last 100 years, suggesting an increase in the rate of climate change over the recent period.

One of the indices, the temperature contrast between the Northern and Southern Hemispheres, shows no significant observed trend in either period, and only small trends in the model simulations. This index was argued to be a useful indicator of the regional cooling due to sulphate aerosols in the Northern Hemisphere [*Michaels and Knappenburger*, 1996; *Santer et al*, 1996b] but the different rates of increase of greenhouse gases and sulphate aerosols appear to lead to substantial variability of this index [*Santer et al*, 1996c]. Also, the two models give different simulated changes in this index, perhaps because it is sensitive to the simulated ocean heat uptake in the Southern Hemisphere.

While we have shown that there are significant changes in four of the indices over the last 40 years and that these changes are consistent with simulations forced with increasing greenhouse gases and sulphate aerosols, we have not considered any other possible climate forcings, such as changing solar irradiance. This is being considered in further work. We are also investigating other possible indices, such as the diurnal temperature range or the temperature contrast between the troposphere and the stratosphere. These were not considered here because observational data for them is not available for the last 100 years.

Acknowledgments. This study was motivated by discussions with a number of colleagues following the IPCC Second Assessment Report. We wish to thank Tony Hirst, Martin Dix and Barrie Hunt at CSIRO Atmospheric Research for making available data from the CSIRO9 simulations and John Mitchell and Simon Tett at the Hadley Centre and the Climate Impacts LINK project at the University of East Anglia for providing data from the HadCM2 simulations. Simulations with HadCM2 were funded by the U.K. Dept. of Environment, Transport and the Regions.

References

Gitelman, A. I., Risbey, J. R., Kass, R. E., and Rosen, R. D. Sensitivity of a meridional temperature gradient index to latitudinal domain. *J. Geophys. Res., 104*, 16709-16717, 1999.

Gordon, H. B., and S. P. O'Farrell, Transient climate change in the CSIRO coupled model with dynamic sea ice. *Mon. Wea. Rev.*, *125*, 875-907, 1997.

Hegerl, G. C. et al., Multi-fingerprint detection and attribution analysis of greenhouse gas, greenhouse gas-plus-aerosol, and solar forced climate change. *Clim. Dynamics*, *13*, 613-634, 1997.

Houghton, J. T., B. A. Callander, and S. K. Varney, (eds.) *Climate Change 1992: The Supplementary Report to the IPCC Scientific Assessment*, CUP, 1992.

Jain, S., U. Lall and M. E. Mann, Seasonality and interannual variations of Northern Hemisphere temperature: Equator-to-pole temperature gradient and ocean-land contrast. *J. Climate*, *12*, 1086-1100, 1999.

Johns, T. C., et al. The second Hadley Centre coupled ocean-atmosphere GCM: Model description, spinup and validation. *Clim. Dynamics*, *13*, 103-134, 1997.

Jones, P. D., Hemispheric surface air temperature variations: A reanalysis and update to 1993. *J. Climate*, *7*, 1794-1802, 1994.

Karl, T. R., R. W. Knight, D. R. Easterling, and R. G. Quayle, Indices of climate change for the United States. *Bull. Amer. Meteor. Soc.*, *77*, 279-292, 1996.

Kaufmann, R. K., and D. I. Stern, Evidence for human influence on climate from hemispheric temperature relations. *Nature*, *388*, 39-44, 1997.

Mann, M. E., and J. Park, Greenhouse warming and changes in the seasonal cycle of temperature: Model versus observations. *Geophys. Res. Lett., 23*, 1111-1114, 1996.

Michaels, P.J., and P.C. Knappenburger, Human effect on global climate? *Nature*, *384*, 523-524, 1996.

Mitchell, J. F. B., and Johns, T. C. On modification of global warming by sulphate aerosols. *J. Climate*, *10*, 245-267, 1997.

Nicholls, N., et al. Observed climate variability and change. In *Climate Change 1995: The science of climate change*, edited by J. T. Houghton et al., pp. 133-192, CUP, Cambridge, UK, 1996.

Parker, D. E., C. K. Folland, and M. Jackson, Marine surface temperature: observed variations and data requirements. *Clim. Change*, *31*, 559-600, 1995.

Piexoto, J. P., and A. H. Oort, *Physics of Climate*, Am. Inst. of Physics, 520 pp, 1992.

Santer, B. D., T. M. L. Wigley, T. P. Barnett, and E. Anyamba, Detection of climate change and attribution of causes. In *Climate Change 1995: The science of climate change*, edited by J. T. Houghton et al., pp. 407-443, CUP, Cambridge, UK, 1996a.

Santer, B. D. et al, A search for human influences on the thermal structure in the atmosphere. *Nature*, *382*, 39-46, 1996b.

Santer, B.D., and others. Human effect on global climate? *Nature*, *384*, 525, 1996c.

Tett, S. F., T. C. Johns, and J. F. Mitchell, Global and regional variability in a coupled AOGCM. *Nature*, *399*, 569-572, 1999.

Thomson, D. J. The seasons, global temperature, precession and CO_2. *Science*, *268*, 59-68, 1995.

D. J. Karoly and K. Braganza, Department of Mathematics and Statistics, Monash University, PO Box 28M, Clayton, VIC 3800, Australia. (email: d.karoly@sci.monash.edu.au)

(Received June 21, 2000; revised October 30, 2000; accepted October 31, 2000.)